Original Article

Maternal-Fetal Medicine®

OPEN

Assessing Coarctation of the Aorta With Fetal Heart Quantification Technology

Jiaojiao Yang[1], Fang Tan[2], Yuqin Shen[1], Yuan Zhao[3], Yan Xia[3], Sihan Fan[4], Xueqin Ji[4,*]

Abstract

Objective: To use fetal heart quantification (*fetal HQ*) technology to compare the coarctation of the aorta (CoA) and normal fetal heart structure and systolic function and to assess whether there are abnormalities in the fetal heart structure and systolic function associated with CoA.

Methods: This prospective cohort study was conducted from May 2020 to December 2022 and involved 18–40-week-old singleton pregnancies and 30 fetuses diagnosed with CoA using fetal echocardiography at the General Hospital of Ningxia Medical University and Peking University First Hospital Ningxia Women's and Children's Hospital, China. The control group contained 60 normal fetuses. The following parameters were recorded and analyzed statistically: four-chamber view (4CV) end-diastolic long diameter, 4CV epicardial–contralateral epicardial transverse maximum diameter, 4CV global sphericity index (GSI), left ventricular (LV) and right ventricular (RV) 24-segment end-diastolic diameter (EDD), 24-segment sphericity index (SI), LV-fractional area change (LV-FAC), LV-longitudinal strain (LV-LS), RV-fractional area change (RV-FAC), RV-longitudinal strain (RV-LS), and LV and RV 24-segment transverse fractional shortening (FS). Measurement data were compared between the two groups using an independent sample *t* test, with $P < 0.05$ indicating statistically significant differences. Moreover, the correlation between gestational age and GSI, LV-FAC, LV-LS, RV-FAC, and RV-LS was assessed.

Results: Within and between observer comparisons of the parameters associated with major cardiac function revealed an intragroup correlation coefficient of >0.9, indicating high consistency, and a coefficient of variable of <1%, indicating low variability. Correlation analysis revealed no obvious correlation between gestational age and GSI, LV-FAC, LV-LS, RV-FAC, and RV-LS. A comparison of the four-chamber morphological structural parameters of the hearts in the two groups revealed that when compared with the control group, the 4CV end-diastolic long diameter was shortened in fetuses in the CoA group and the epicardial–contralateral epicardial transverse maximum diameter was wider, while the GSI was lower ($P < 0.05$). A comparison of the LV and RV morphological structure parameters between the two groups revealed that when compared with the control group, the LV's 24-segment EDD was smaller in the CoA group, the RV's 24-segment EDD was greater in the control group, the SI of the LV's segments 16–24 was greater than in the control group, and the SI of the RV's segments 7–24 was less than in the control group (all $P < 0.05$). When compared with fetuses in the control group, the LV's segments 16–24 were greater in the CoA group, whereas the RV's segment 6–24 was smaller ($P < 0.05$). When compared with the control group, LV-FAC, RV-FAC, and LS were lower in the CoA group ($P < 0.05$). The FS of the LV segments 1–24 and the FS of the RV segments 1–16 were smaller in the CoA group than in the normal group ($P < 0.05$).

Conclusion: *Fetal HQ*, a new simple technique that offers rapid analysis and high repeatability, can quantitatively evaluate structural and systolic function changes in fetuses with CoA.

Keywords: Fetal heart; Quantitative analysis technology; Fetal HQ software; Coarctation of the aorta; Spherical index; Systolic function

Introduction

Coarctation of the aorta (CoA), which refers to the congenital constriction of the descending aortic arch, mainly occurs at the distal end of the left subclavian artery and near the insertion point of the ductus arteriosus,[1] and accounts for 4%–6% of congenital heart disease.[2–4] Although CoA can manifest as a simple disease, it may also occur along with other cardiac malformations, including ventricular septal defect, aortic valve bicuspid malformation, subaortic valve stenosis, and mitral valve malformation. In cases of uncomplicated CoA, 50% of untreated individuals die within 10 years of life, whereas 90% die before the age of 50 years.[5] Its causes of death include congestive heart failure, aortic rupture, bacterial endocarditis, and intracranial hemorrhage, which account for 26%, 21%, 18%, and 12% of the deaths, respectively.[6] However, prenatal CoA diagnosis is associated with low sensitivity and a high false-positive rate.[7]

Recently, spot-tracking technology has been used to develop fetal heart quantification (*fetal HQ*) software for the automatic assessment of fetal heart structure and systolic function. This ultrasound technique analyzes fetal heart

Supplemental Digital Content is available for this article. Direct URL citations appear in the printed text and are provided in the HTML and PDF versions of this article on the journal's website (www.maternalfetalmedicine.org).

[1]Department of Obstetrics and Gynecology Center, General Hospital of Ningxia Medical University, Yinchuan, Ningxia 750003, China; [2]Ultrasound Medicine Department, Xian Yang Central Hospital, Xianyang, Shaanxi 712099, China; [3]Ultrasound Medicine Department, Peking University First Hospital Ningxia Women's and Children's Hospital (Ningxia Hui Autonomous Region Maternal and Child Health Hospital), Yinchuan, Ningxia 750002, China; [4]Ningxia Medical University, Yinchuan, Ningxia 750004, China.

** Corresponding author: Xueqin Ji, Ningxia Medical University, Yinchuan, Ningxia 750004, China. E-mail: jinian54@163.com*

Maternal-Fetal Medicine (2024) 6:3

Received: 20 July 2023 / Accepted: 15 April 2024

First online publication: 3 July 2024

http://dx.doi.org/10.1097/FM9.0000000000000231

function using the classic two-dimensional (2D) speck tracking imaging technology to quantitatively examine the morphology and contractile function of fetal left and right ventricles based on a 2D dynamic four-chamber heart section. At the same time, a 24-segment analysis report of the biventricular end-diastolic ventricular diameter, short-axis shortening rate, and end-diastolic spherical index is generated, Moreover, comprehensive fetal heart function assessment can be conducted based on a combination of several qualitative and quantitative indicators, such as the Z-score.[8–19] Here, we sought to determine the application value of *fetal HQ* in the evaluation of cardiac structure and systolic function in fetal CoA and to develop a new method for the clinical evaluation of fetal heart function in fetuses with CoA.

Materials and methods

Study participants

This prospective cohort study involved pregnant women who underwent prenatal ultrasound examination from May 2020 to December 2022 at the Department of Obstetrics and Gynecology, General Hospital of Ningxia Medical University and the Ultrasound Department of Peking University First Hospital Ningxia Women's and Children's Hospital. The gestational age (GA) was determined using ultrasound and calculated based on the last menstrual period. Biological parameters, including biparietal diameter, head circumference, abdominal circumference, femur length, and estimated fetal weight, were measured to assess their consistency with the GA.

Inclusion and exclusion criteria

Eligibility for participation in this study was determined based on the following inclusion criteria: individuals aged 18 years or older, GA between 18 and 40 weeks, a prior history of regular menstrual cycles, and a singleton pregnancy as confirmed by brightness mode ultrasonography. Exclusion criteria comprised the presence of severe fetal cardiac anomalies, including but not limited to left heart dysplasia syndrome, complete transposition of the great arteries, endocardial cushion defects, isolated single ventricle defects, tetralogy of Fallot, and persistent truncus arteriosus. Additionally, potential participants were excluded if they presented with any fetal heart abnormalities, discernible internal or external fetal abnormalities, or if the pregnant woman had preexisting conditions such as diabetes, cardiac disorders, hypertension, or other pregnancy-associated complications.

Prenatal diagnosis of fetal CoA

Fetal CoA was diagnosed according to the guidelines established by the Obstetrics and Gynecology Ultrasound Group of the Ultrasound Medicine Branch of the Chinese Medical Association.[6] Based on the four-chamber cardiac section, CoA was diagnosed by the presence of right ventricle enlargement, a relative left ventricle decrease, and a right ventricle–left ventricle transverse diameter of >1.6. Based on the left and right outflow tract section, it is characterized by a pulmonary annulus–aortic annulus inner diameter of >1.6. The long axis section of the aortic arch or the three-vessel tracheal section exhibits a narrow transverse aortic arch or narrow aortic isthmus, respectively, with the Z-value of the inner isthmus diameter being <–2. In the aortic arch, the color Doppler flow imaging exhibits a reduced or even reversed blood flow signal. Based on the pulse Doppler, blood flow at the stenosis is not significantly accelerated, but abnormalities that manifest as an increased proportion of diastolic blood flow and an increased flow rate may occur.

Instruments

GE Voluson E8 and E10 color Doppler ultrasounds, equipped with C6-1 and C9-2 probes, and utilizing the *fetal HQ* software, were employed at frequencies ranging from 1 to 6 MHz and 2 to 9 MHz, respectively. Pregnant women were positioned in supine or lateral positions for routine 2D examination and image acquisition. They then underwent routine 2D ultrasonography in obstetrics to acquire data on fetal biological characteristic parameters, including head circumference, biparietal diameter, abdominal circumference, and femur length, as well as to determine the GA and whether there are potential extracardiac malformations. Next, they underwent fetal echocardiography in which 2D dynamic images in the four-chamber view (4CV) were taken at an image acquisition frame rate of ≥80 frames/second. Various interference factors, including the thickness of the abdominal wall fat layer in pregnant women, GA, fetal positioning or movement, and the volume of amniotic fluid, were excluded. By optimizing the images to enhance and clearly display the blood pool–endocardium border, stable dynamic-images of the fetal four-chamber heart were obtained.

Fetal heart quantitative analysis

For *fetal HQ* analysis, images were exported into GE Voluson E10 equipped with the *fetal HQ* software. In the *fetal HQ* system, the end-diastolic basal-apical length (4CV-ED-L, the length from the atrium's posterior wall to the apical epicardium) and transverse width (4CV-ED-TW, the maximum transverse width of the heart with 4CV end-diastolic) were measured from the 4CV to calculate the global sphericity index (GSI) of the four-chamber heart (Fig. 1A). Next, the motion mode ultrasound, combined with the opening and closing status of each valve on the 2D four-chamber dynamic image, was used to determine the end-diastolic and end-systolic stages (Fig. 1B). Click on the junction of the atrioventricular valve and the ventricular septum, the junction of the atrioventricular valve and the ventricular free wall, and the apical endocardium (Fig. 1C left: three red dots), and the *fetal HQ* software can automatically detect and outline the endocardial boundary of the ventricle. The left and right ventricle endocardial boundaries were automatically traced at the junction of the mitral valve, tricuspid valve, and ventricle, as well as the apex of the left and right ventricles (Fig. 1D). Finally, the *fetal HQ* software was used to automatically divide the left and right ventricles into 24 segments, with segments 1–8, 9–16, and 17–24 indicating the basal, middle, and apical segments, respectively, which were used to obtain the left and right ventricles' 24-segment end-diastolic diameter (EDD), 24-segment sphericity index (SI), left ventricle-fractional area change (LV-FAC), left ventricle longitudinal strain (LV-LS), right ventricle-fractional area change (RV-FAC), right ventricular longitudinal strain

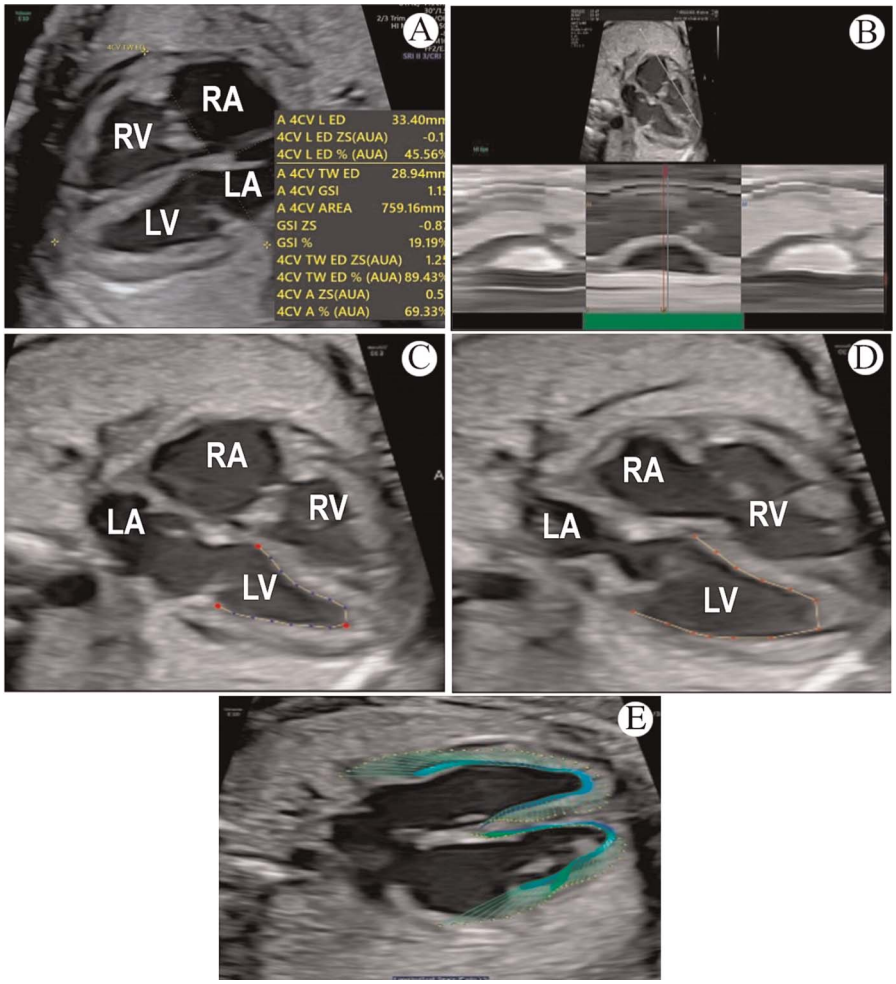

Figure 1. Fetal HQ software operation process. A The four-chamber GSI at end-diastole measured by fetal HQ. B Identification of an end-diastole and an end-systole using M-mode ultrasound combined with two-dimensional four-chamber dynamic images of the valve opening and closing states. C&D Sampling points are placed at the junction of the mitral valve, tricuspid valve and ventricle and at the apex of the left ventricle and right ventricle. E Left and right ventricles divided into 24 segments by fetal HQ. A: Area of the heart; AUA: Average ultrasound age; 4CV L ED: 4 chamber view length end-diastole; 4CV TW ED: 4-chamber view transverse width end-diastole; GSI: Global sphericity index; HQ: Heart quantification; M-mode: Motion mode; LA: Left atrium; LV: Left ventricle; RA: Right atrium; RV: Right ventricle; ZS: Z-score.

(RV-LS), and left and right ventricular 24-segment transverse fractional shortening (FS) (Fig. 1E).

Statistical analysis

Statistical analyses were done using SPSS 26.0 statistical software (IBM). Normally distributed data are presented as mean ± standard deviation (*SD*). For normally distributed data, differences between two groups were compared using an independent sample *t* test. A *P* value of <0.05 indicates statistically significant differences. The correlation between GA and GSI, LV-FAC, LV-LS, RV-FAC, and RV-LS was assessed and the data were visualized on scatter plots. Pearson correlation analysis was used for non-normally distributed data, whereas Spearman correlation analysis was used for non-normally distributed data ($|r| \geq 0.8$, $0.5 \leq |r| < 0.8$, $0.3 \leq |r| < 0.5$, $|r| < 0.3$, or $r = 0$ indicate high, moderate, low, and weak or no correlation, respectively). To evaluate intraobserver consistency, 20 fetuses that underwent the first *fetal HQ* analysis were randomly selected a month later and reanalyzed by the same examiner. To assess interobserver agreement, 20 fetuses were randomly selected and analyzed by a different trained sonographer. Intragroup correlation coefficient (ICC) values of 0.4–<0.6, 0.6–<0.8, and 0.8–1.0 indicate moderate, strong, and very strong degrees, respectively. Inter- and intraobserver variability were assessed using the coefficient of variation (CoV), with a CoV of <10% indicating low variability.

Ethical approval

All study participants were informed about the reliability and limitations of the examination used in this study and gave signed informed consent to undergo fetal ultrasonography. This study was approved by the ethics committees of the General Hospital of Ningxia Medical University (approval number [202020]0520B) and Peking University First Hospital Ningxia Women's and Children's Hospital (approval number KJ-LL-2022-26). The study adhered to the 2013 *Declaration of Helsinki* guidelines.

Results

Based on follow-up results, 38 cases of prenatal fetal CoA were identified and of these, 30 (the CoA group) were consistent with the postnatal echocardiography results, and eight cases were excluded because they had normal postnatal cardiac ultrasound results. The control group contained 60 healthy pregnant women who underwent fetal echocardiography at two hospitals during the same period.

Consistency analysis

Intra- and interobserver analysis of the fetuses' main cardiac function-related parameters revealed an ICC of >0.9, indicating strong consistency. Moreover, all CoVs were <1%, indicating low variability (Table 1).

Correlation analysis

The results of the correlation analysis between fetal GA and GSI, LV-FAC, LV-LS, RV-FAC, and RV-LS in the CoA and control groups were visualized using a scatter diagram of the correlation between GA and each variable (Fig. 2A–J, http://links.lww.com/MFM/A50). This analysis revealed no significant correlation between GA and GSI, LV-FAC, LV-LS, RV-FAC, and RV-LS (Table 2).

Comparison of fetal four-chamber heart morphological parameters between the two groups

The morphological parameters of the fetal four-chamber heart in the CoA and control groups were measured using the fetal *HQ* software to obtain GSI. A comparison of the four-chamber morphological structural parameters of the hearts in the two groups revealed that when compared with the control group, 4CV end-diastolic long diameter, 4CV epicardial–contralateral epicardial transverse maximum diameter and GSI were statistically significant ($P < 0.05$) (Table 3).

Comparison of left and right ventricle morphological parameters between the two groups

When compared with the fetuses in the control group, the EDD of the LV's segments 1–24 was smaller in the CoA group, whereas the EDD of the RV's segments 1–24 was greater in the CoA group (all $P < 0.05$, Table 4). When compared with fetuses in the control group, the SI of the LV's segments 16–24 were greater in the CoA group, whereas the RV's segment 6–24 was smaller (all $P < 0.05$, Table 5).

Table 1

Interobserver and intraobserver consistency analysis.

	Interobserver			Intraobserver		
Parameter	ICC	95% *CI*	CoV (%)	ICC	95% *CI*	CoV (%)
GSI	0.980	0.940–0.990	0.8	0.961	0.890–0.987	0.6
LV-LS	0.937	0.826–0.987	0.3	0.957	0.874–0.958	0.3
RV-LS	0.988	0.967–0.996	0.4	0.937	0.825–0.978	0.3
LV-FAC	0.961	0.890–0.987	0.6	0.985	0.956–0.995	0.2
RV-FAC	0.910	0.755–0.969	0.9	0.930	0.788–0.972	0.2

CI: Confidence interval; CoV: Coefficient of variation; FAC: Fractional area change; GSI: Global sphericity index; ICC: Intraclass correlation coefficient; LS: Longitudinal strain; LV: Left ventricle; RV: Right ventricle.

Table 2

Correlation between GA and cardiac function parameters.

Group	Variable	*r*	*P*
CoA group ($n = 30$)	GSI	−0.111	0.559
	LV-FAC	−0.341	0.065
	LV-LS	0.239	0.203
	RV-FAC	0.216	0.251
	RV-LS	−0.199	0.293
Control group ($n = 60$)	GSI	−0.094	0.622
	LV-FAC	−0.328	0.077
	LV-LS	0.239	0.203
	RV-FAC	0.175	0.354
	RV-LS	−0.220	0.243

CoA: Coarctation of the aorta; FAC: Fractional area change; GA: Gestational age; GSI: Global sphericity index; LV: Left ventricle; LS: Longitudinal strain; RV: Right ventricle.

Comparison of fetal systolic function parameters between the two groups

When compared with the control group, LV-FAC, RV-FAC, and LS values in the CoA group were significantly different. ($P < 0.05$, Table 6). Specifically, the LS values in the CoA group were higher (less negative) at −13.55% ± 1.57%, compared to −19.61% ± 0.81% in the control group. The FS of the LV segments 1–24 and the FS of the RV segments 1–16 were smaller in the CoA group than in the normal group (all $P < 0.05$, Table 7).

Discussion

The main ultrasound fetal congenital heart disease manifestations are changes in cardiac morphology and function. Different congenital heart disease types appear differently on ultrasound images. Because of cardiac structure and hemodynamic changes, the myocardium undergoes compensatory changes to maintain normal cardiac function, resulting in a remodeled cardiac structure and an abnormal cardiac structure and systolic function. The timely and accurate diagnosis of fetal cardiac dysfunction, along with early intervention, can effectively improve the fetus's perinatal outcomes. Therefore, the early detection and prenatal diagnosis of fetal cardiac dysfunction have important clinical implications.

This study shows that GA did not correlate significantly with morphological and systolic function parameters,

Table 3

Comparison of the four-chamber heart size and overall sphericity index in the CoA group *vs.* the control group.

Parameter	CoA group ($n = 30$) (mean ± *SD*)	Control group ($n = 60$) (mean ± *SD*)	*t*	*P*
4CV-ED-L (mm)	35.21 ± 1.44	38.79 ± 0.76	−2.43	0.017
4CV-ED-TW (mm)	40.27 ± 0.84	34.15 ± 0.76	4.97	<0.001
4CV-GSI (%)	1.05 ± 0.03	1.14 ± 0.01	−3.21	0.002

4CV: 4-chamber view; CoA: Coarctation of the aorta; ED: End-diastolic; GSI: Global spherical index; L: Maximum length of the epicardium from the posterior wall of the atrium to the apical segment; TW: Transverse width (the maximum length between transverse epicardia).

Table 4

Comparison of left and right ventricular EDD values in the CoA group *vs.* the control group.

Segment	LV-EDD (%, mean ± *SD*)				RV-EDD (%, mean ± *SD*)			
	CoA group (*n* = 30)	Control group (*n* = 60)	*t*	*P*	CoA group (*n* = 30)	Control group (*n* = 60)	*t*	*P*
1	10.10 ± 0.46	11.77 ± 0.27	–3.31	0.001	13.74 ± 0.77	12.20 ± 0.38	2.48	0.015
2	9.99 ± 0.45	11.78 ± 0.27	–3.61	0.003	14.18 ± 0.80	12.36 ± 0.37	2.37	0.021
3	9.88 ± 0.44	11.67 ± 0.27	–3.85	<0.001	14.29 ± 0.80	12.51 ± 0.37	2.31	0.024
4	9.76 ± 0.44	11.75 ± 0.27	–4.05	<0.001	14.24 ± 0.79	12.62 ± 0.37	2.11	0.038
5	9.63 ± 0.43	11.69 ± 0.27	–4.19	<0.001	14.20 ± 0.79	12.66 ± 0.38	2.02	0.046
6	9.47 ± 0.43	11.59 ± 0.27	–4.31	<0.001	14.14 ± 0.77	12.60 ± 0.37	2.03	0.045
7	9.30 ± 0.43	11.45 ± 0.27	–4.41	<0.001	14.09 ± 0.77	12.45 ± 0.37	2.18	0.032
8	9.12 ± 0.42	11.28 ± 0.27	–4.45	<0.001	13.92 ± 0.76	12.24 ± 0.36	2.27	0.026
9	8.95 ± 0.42	11.10 ± 0.27	–4.45	<0.001	13.75 ± 0.76	11.97 ± 0.35	2.24	0.017
10	8.79 ± 0.43	10.92 ± 0.27	–4.40	<0.001	13.40 ± 0.73	11.66 ± 0.35	2.46	0.016
11	8.62 ± 0.43	10.73 ± 0.27	–4.34	<0.001	13.01 ± 0.70	11.32 ± 0.34	2.45	0.016
12	8.44 ± 0.43	10.54 ± 0.27	–4.28	<0.001	12.60 ± 0.67	10.95 ± 0.33	2.48	0.015
13	8.22 ± 0.43	10.33 ± 0.27	–4.26	<0.001	12.09 ± 0.64	10.55 ± 0.33	2.38	0.019
14	7.97 ± 0.44	10.11 ± 0.28	–4.31	<0.001	11.59 ± 0.61	10.12 ± 0.32	2.37	0.020
15	7.68 ± 0.43	9.88 ± 0.28	–4.43	<0.001	11.07 ± 0.57	9.65 ± 0.31	2.37	0.020
16	7.38 ± 0.43	9.63 ± 0.27	–4.61	<0.001	10.50 ± 0.53	9.15 ± 0.30	2.38	0.020
17	7.07 ± 0.41	9.38 ± 0.26	–4.88	<0.001	9.88 ± 0.49	8.59 ± 0.30	2.37	0.020
18	6.75 ± 0.40	9.10 ± 0.25	–5.52	<0.001	9.17 ± 0.45	7.99 ± 0.28	2.33	0.022
19	6.38 ± 0.38	8.73 ± 0.23	–5.56	<0.001	8.37 ± 0.40	7.31 ± 0.27	2.21	0.031
20	5.88 ± 0.36	8.14 ± 0.21	–5.77	<0.001	7.44 ± 0.35	6.52 ± 0.25	2.16	0.034
21	5.16 ± 0.32	7.20 ± 0.19	–5.83	<0.001	6.35 ± 0.29	5.56 ± 0.22	2.11	0.038
22	4.15 ± 0.26	5.82 ± 0.16	–5.81	<0.001	5.09 ± 0.24	4.39 ± 0.18	2.29	0.025
23	2.90 ± 0.18	4.09 ± 0.11	–5.77	<0.001	3.68 ± 0.18	3.03 ± 0.13	2.91	0.005
24	1.49 ± 0.10	2.10 ± 0.06	–5.74	<0.001	2.16 ± 0.13	1.55 ± 0.07	4.70	<0.001

Segments 1–8 indicating basal segment; segments 9–16 indicating middle segment; segments 17–24 indicating apical segment.

CoA: Coarctation of the aorta; EDD: End-diastolic diameter; LV: Left ventricle; RV: Right ventricle; *SD*: Standard deviation.

which indicates that the heart's geometry, systolic function, and ventricles were relatively stable and that the heart's shape and systolic function did not increase with the GA but changed gradually. Based on echocardiographic data from 154 normal fetuses, Clavero Adell *et al.*[20] found that when compared with the right ventricle, the left ventricle's strain value was higher. This indicates that the SI and strain rate are independent of GA when evaluating myocardial function and are more convenient to use.

The heart, one of the most important organs during fetal growth and development, continuously circulates nutrients from the mother throughout the fetus. However, the fetal heart is extremely fragile and various factors, such as the umbilical cord around the neck, maternal malnutrition, and long-term radiation exposure, may damage heart function, resulting in structure remodeling and a severe impairment of myocardial cell regeneration. This can have a life-long impact on affected children.[19] Fetal SI, the ratio between the heart's long and transverse diameters was first proposed by DeVore *et al.*[11] in 2016 and is used to quantify the degree of cardiac remodeling and reflects the geometric shape of the ventricles, atria, and the entire heart.

Fetal HQ technology can determine the four-chamber heart GSI as well as divide the left and right ventricles into 24 segments (from the base to the apex), automatically calculate the 24 segments' EDDs and evaluate each segment's size and shape. When compared with the control group, fetal heart morphology was changed in the CoA group, with the heart appearing more spherical, indicating increased width and decreased length. When compared with the normal group, the EDD of all left ventricle segments was smaller in the CoA group, whereas the SI of the apical segment increased. When compared with the normal group, the EDD of all right ventricle segments was greater in the CoA group, whereas the SI of some basal segments (segment 6–8) and all intermediate and apical segments was smaller, which is consistent with the findings by DeVore *et al.*[21,22] If the arterial ductus theory can explain this series of cardiac morphological changes, it may be that during progressive CoA development, blood flow is not smooth because of arch stenosis, resulting in a significant increase in the left ventricle afterload, decreases in blood flow from the left atrium to the left ventricle and from the right atrium into the left atrium through the foramen ovale, a left ventricle end-diastolic volume decrease, a greater SI value than in the normal group, and an elongated left ventricle. Moreover, because fetal CoA is mainly of the preductal type, the existence of the ductus arteriosus and progression in aortic arch narrowing causes blood flow through the right ventricle to the pulmonary artery and ductus arteriosus to increase significantly. Because of the right ventricular hypervolemia, the SI is smaller in the CoA group than in the normal group, and the right ventricular part of the basal segment and the entire middle and the apical segments are spherical, which causes the ventricular septum to expand

Table 5

Comparison of the 24-segment SI of the left and right ventricle between the fetuses of the CoA group and the fetuses of the control group.

Segment	LV-SI (%, mean ± *SD*)				RV-SI (%, mean ± *SD*)			
	CoA group (*n* = 30)	Control group (*n* = 60)	*t*	*P*	CoA group (*n* = 30)	Control group (*n* = 60)	*t*	*P*
1	1.73 ± 0.08	1.75 ± 0.05	−0.22	0.837	1.36 ± 0.06	1.49 ± 0.04	−1.73	0.089
2	1.74 ± 0.08	1.75 ± 0.05	−0.02	0.986	1.34 ± 0.06	1.47 ± 0.04	−1.78	0.078
3	1.76 ± 0.08	1.75 ± 0.05	0.18	0.859	1.32 ± 0.06	1.45 ± 0.04	−1.83	0.070
4	1.78 ± 0.08	1.75 ± 0.05	0.38	0.702	1.30 ± 0.06	1.44 ± 0.04	−1.86	0.063
5	1.81 ± 0.08	1.76 ± 0.05	0.56	0.582	1.29 ± 0.06	1.43 ± 0.04	−1.99	0.053
6	1.84 ± 0.08	1.77 ± 0.05	0.74	0.462	1.28 ± 0.06	1.44 ± 0.04	−2.23	0.028
7	1.87 ± 0.08	1.79 ± 0.05	0.89	0.377	1.28 ± 0.05	1.46 ± 0.04	−2.48	0.015
8	1.91 ± 0.09	1.82 ± 0.05	1.02	0.307	1.29 ± 0.05	1.48 ± 0.04	−2.67	0.009
9	1.95 ± 0.09	1.85 ± 0.05	1.12	0.272	1.31 ± 0.05	1.52 ± 0.04	−2.79	0.007
10	1.99 ± 0.09	1.88 ± 0.05	1.18	0.239	1.34 ± 0.06	1.56 ± 0.05	−2.83	0.006
11	2.04 ± 0.10	1.92 ± 0.05	1.23	0.223	1.38 ± 0.06	1.61 ± 0.05	−2.82	0.006
12	2.09 ± 0.10	1.96 ± 0.05	1.31	0.195	1.43 ± 0.06	1.67 ± 0.05	−2.79	0.007
13	2.15 ± 0.11	2.00 ± 0.05	1.44	0.156	1.49 ± 0.06	1.73 ± 0.06	−2.76	0.007
14	2.24 ± 0.12	2.05 ± 0.06	1.63	0.106	1.55 ± 0.06	1.81 ± 0.06	−2.76	0.007
15	2.33 ± 0.13	2.10 ± 0.06	1.87	0.066	1.63 ± 0.06	1.91 ± 0.06	−2.79	0.006
16	2.44 ± 0.14	2.16 ± 0.06	2.14	0.035	1.71 ± 0.06	2.02 ± 0.07	−2.83	0.006
17	2.55 ± 0.14	2.22 ± 0.06	2.48	0.015	1.82 ± 0.06	2.15 ± 0.07	−2.87	0.005
18	2.66 ± 0.14	2.27 ± 0.06	2.89	0.005	1.97 ± 0.07	2.32 ± 0.08	−2.91	0.004
19	2.80 ± 0.14	2.36 ± 0.06	3.35	0.001	2.16 ± 0.07	2.54 ± 0.09	−2.89	0.005
20	3.04 ± 0.15	2.53 ± 0.06	3.75	<0.001	2.45 ± 0.08	2.86 ± 0.10	−2.78	0.007
21	3.46 ± 0.16	2.86 ± 0.07	4.01	<0.001	2.91 ± 0.09	3.37 ± 0.12	−2.58	0.012
22	4.30 ± 0.19	3.54 ± 0.09	4.15	<0.001	3.74 ± 0.12	4.30 ± 0.16	−2.37	0.020
23	6.15 ± 0.27	5.06 ± 0.12	4.21	<0.001	5.46 ± 0.18	6.26 ± 0.24	−2.22	0.029
24	11.97 ± 0.53	9.83 ± 0.24	4.24	<0.001	10.75 ± 0.37	12.31 ± 0.49	−2.13	0.036

Segments 1–8: basal segment, segments 9–16: middle segment, segments 17–24: apical segment.

CoA: Coarctation of the aorta; LV: Left ventricle; RV: Right ventricle; SI: Spherical index; *SD*: Standard deviation.

to the left ventricular side, resulting in a smaller left ventricular volume and a corresponding increase in left ventricular pressure to more effectively balance the left ventricular afterload hypertension.[23] According to the hemodynamic theory, this series of changes may be because of various factors, including the combined oval valve length and foramen ovale blood flow restriction, resulting in fetal right atrial volume overload, right heart enlargement, tricuspid regurgitation, decreased left heart blood flow, left heart shrinkage, asymmetrical left ventricular size, secondary to fetal period blood flow into the aortic arch, and a narrow aortic isthmus. In a study involving 35 late-pregnancy fetuses with restricted blood flow in the foramen ovale, Liu *et al*.[24] showed that the left ventricle was flatter and the right ventricle's basal and middle segments were close to spherical, which is similar to the ventricular morphological changes observed in this study in fetuses with CoA. Because nine of the fetal CoA cases included in this study also had foramen ovale blood flow restriction, the author speculated that CoA was secondary to foramen ovale blood flow restriction, although it is not possible to draw firm conclusions from the few cases that were included. In a study involving 25 fetal cases of left ventricular outflow tract obstruction (LVOTO), Zhan *et al*.[25] found that in fetuses with LVOTO, the four-chamber heart was spherical, had an increased area and width, the right ventricle was more spherical because of increased transverse diameter and the left ventricle was a flat chamber. This is consistent with the findings of this study, indicating that heart hemodynamic changes caused by diseases like LVOTO are the same. Therefore, the changes affecting the heart and ventricular morphology are also the same, although further research is needed to determine which type of LVOTO disease specifically impacts

Table 6

Comparison of the 24-segment SI of the left and right ventricles between the fetuses of the CoA group and the fetuses of the control group.

Parameter	LV (mean ± *SD*)				RV (mean ± *SD*)			
	CoA group (*n* = 30)	Control group (*n* = 60)	*t*	*P*	CoA group (*n* = 30)	Control group (*n* = 60)	*t*	*P*
FAC (%)	27.39 ± 2.97	39.86 ± 1.32	−4.45	<0.001	20.44 ± 1.47	26.34 ± 1.49	−2.50	0.014
LS (%)	−13.55 ± 1.57	−19.61 ± 0.81	3.80	<0.001	−11.17 ± 1.62	−14.59 ± 0.87	2.04	0.044

CoA: Coarctation of the aorta; FAC: Fractional area change, LS: Longitudinal strain; LV: Left ventricle, RV: Right ventricle; SI: Sphericity index; *SD*: Standard deviation.

Table 7

Comparison of the left and right ventricles' 24-segment FS in the CoA group *vs*. the control group.

Segment	LV-FS (%, mean ± *SD*)				RV-FS (%, mean ± *SD*)			
	CoA group (*n* = 30)	Control group (*n* = 60)	*t*	*P*	CoA group (*n* = 30)	Control group (*n* = 60)	*t*	*P*
1	7.33 ± 2.69	14.96 ± 1.10	–3.11	0.003	5.50 ± 2.49	13.75 ± 1.25	–3.31	0.001
2	8.50 ± 2.62	16.10 ± 1.08	–3.17	0.002	5.61 ± 2.44	13.91 ± 1.17	–3.48	0.001
3	9.70 ± 2.57	17.24 ± 1.09	–3.17	0.002	6.04 ± 2.35	14.05 ± 1.11	–3.51	0.001
4	10.93 ± 2.54	18.48 ± 1.12	–3.16	0.002	6.08 ± 2.35	14.16 ± 1.08	–3.59	0.001
5	12.22 ± 2.50	19.87 ± 1.15	–3.20	0.002	6.24 ± 2.34	14.23 ± 1.06	–3.59	0.001
6	13.57 ± 2.45	21.49 ± 1.18	–3.30	0.001	6.63 ± 2.29	14.27 ± 1.05	–3.48	0.001
7	14.93 ± 2.40	23.24 ± 1.21	–3.45	0.001	7.12 ± 2.28	14.27 ± 1.07	–3.23	0.002
8	16.26 ± 2.39	25.02 ± 1.25	–3.59	0.001	7.69 ± 2.27	14.19 ± 1.11	–2.90	0.005
9	17.49 ± 2.40	26.68 ± 1.29	–3.70	<0.001	7.57 ± 2.32	14.03 ± 1.17	–2.77	0.007
10	18.54 ± 2.43	28.12 ± 1.32	–3.77	<0.001	7.63 ± 2.37	13.75 ± 1.25	–2.51	0.014
11	19.40 ± 2.50	29.36 ± 1.35	–3.84	<0.001	4.79 ± 2.63	13.38 ± 1.34	–3.25	0.002
12	20.04 ± 2.58	30.50 ± 1.37	–3.94	<0.001	4.85 ± 2.63	12.98 ± 1.43	–2.96	0.004
13	20.47 ± 2.68	31.60 ± 1.39	–4.09	<0.001	4.74 ± 2.61	12.61 ± 1.53	–2.77	0.007
14	20.69 ± 2.81	32.74 ± 1.40	–4.30	<0.001	4.61 ± 2.54	12.32 ± 1.63	–2.64	0.010
15	20.76 ± 2.95	33.89 ± 1.43	–4.53	<0.001	4.64 ± 2.55	12.03 ± 1.72	–2.44	0.017
16	20.69 ± 3.09	34.97 ± 1.47	–4.74	<0.001	4.64 ± 2.60	11.64 ± 1.81	–2.22	0.029
17	20.47 ± 3.20	35.93 ± 1.53	–4.95	<0.001	4.81 ± 2.55	11.03 ± 1.88	–1.94	0.056
18	20.11 ± 3.22	36.70 ± 1.60	–5.17	<0.001	4.53 ± 2.34	10.10 ± 1.91	–1.75	0.083
19	19.72 ± 3.21	37.26 ± 1.68	–5.34	<0.001	2.96 ± 2.29	8.89 ± 1.98	–1.84	0.070
20	19.41 ± 3.21	37.67 ± 1.77	–5.42	<0.001	3.10 ± 2.19	7.52 ± 2.13	–1.30	0.197
21	19.24 ± 3.23	37.95 ± 1.84	–5.41	<0.001	1.76 ± 2.09	6.13 ± 2.40	–1.18	0.242
22	19.19 ± 3.26	38.13 ± 1.90	–5.35	<0.001	2.34 ± 1.93	5.01 ± 2.70	–0.66	0.513
23	19.18 ± 3.29	38.26 ± 1.94	–5.31	<0.001	2.25 ± 1.90	4.21 ± 2.95	–0.45	0.657
24	19.19 ± 3.31	38.32 ± 1.96	–5.28	<0.001	0.50 ± 1.89	3.73 ± 3.12	–0.46	0.646

Segments 1–8: basal segments, segments 9–16: intermediate segments, segments 17–24: apical segments.

CoA: Coarctation of the aorta; FS: Fractional shortening; LV: Left ventricle; RV: Right ventricle; *SD*: Standard deviation.

each ventricle segment. Liu *et al*.[26] found that GSI did not differ significantly between groups with and without CoA, probably because of other cardiac abnormalities in fetuses without CoA.

Because fetal heart morphological changes are usually secondary to heart function changes, it is important to monitor heart function changes using ultrasound in CoA. The left ventricular ejection fraction, atrioventricular valve primary and pulmonary artery blood flow, atrioventricular valve E peak forward flow rate, A peak, and their ratios have been previously used to assess fetal cardiac function.[20] The clinical assessment of cardiac function using speckle-tracking echocardiology has begun in recent years and it is increasingly used to assess adult cardiac function.[27–31] Moreover, it has value in the early diagnosis and prognosis of various conditions, including myocardial infarction, diabetes, and hypertension, and gradually, it is being used to evaluate cardiac function in fetuses with restricted blood flow in the foramen ovale channel,[24] LVOTO,[25] anemia,[32] and hypertension.[33]

Fetal HQ can determine LV-FAC, RV-FAC, LV-LS, and RV-LS and divide the ventricles into 24 segments and analyze each segment's FS changes. This study shows that when compared with the control group, the left ventricle's overall systolic function, longitudinal contractile function, and lateral contractile function were inhibited in fetuses in the CoA group, whereas these parameters were inhibited in the right ventricle's basal and middle segments, which is consistent with the findings of DeVore *et al*.[21,22] Xu *et al*.[34] reported reduced fetal ventricular FAC in the CoA group, and a study by Liu *et al*.[26] that involved 122 fetuses with CoA reported that LV-FAC and LV-LS were reduced in fetuses with CoA, although there were no significant changes in RV-FAC and RV-LS. Fetal cardiomyocytes are susceptible to hypoxia, which leads to sarcomere shortening in myocardial cells, which are an important component of myocardial contraction.[35,36] However, remodeling the myocardium adversely affects its contractile function. One mechanism of maintaining the cardiac output required for fetal growth is to change the size, shape, and contractile function of the whole fetal heart, as well as the ventricles.[37,38] We hypothesize that the fetal heart's transverse diameter becomes wider in the early stages of mild hypoxia but the heart's apex-to-base length does not change significantly, and that this change can maintain stroke volume.[39]

Fetal hemodynamic changes during CoA increase the right heart transverse diameter to close to a spherical shape and decrease the left heart transverse diameter to close to flat. Because the endocardium is most sensitive to ischemia and hypoxia, and the overall LS mainly reflects endocardial changes, significant ventricular morphological changes change the endocardium, and the overall fetal ventricle LS decreases. Changes in the fetal heart's transverse diameter change the transverse contractile function of the left and right ventricles, resulting in aortic arch narrowing, a wider right ventricle transverse diameter, and a more significant FS reduction. However, although the width of the left ventricle is

significantly reduced, FS is not obvious and when the latter occurs, it indicates a significant reduction in lateral myocardial movement, and the transverse contractile function is significantly inhibited. Moreover, when ventricles are dilated, a transverse diameter increase may lead to a decrease in the calculated value, resulting in outliers. Therefore, when the transverse shortening rate changes substantially, clinicians should consider assessing fetal cardiac function further using other diagnostic tools. If heart function continues to deteriorate in CoA cases in the third trimester, the fetal ventricular area becomes inconsistent because the ventricular area change rate is later than the rates of the overall LS change and lateral shortening. Therefore, when the aortic arch narrows, the longitudinal and lateral contractile functions of the fetuses are significantly reduced, which inevitably decreases the fetus's overall contractile function.

This study has several advantages. First, the images subjected to quantitative analysis are simple and only require the collection of the fetal four-chamber dynamic map. Moreover, four-chamber cardiac sections are routinely examined by fetal echocardiogram sections, the success rate is nearly 100%, and the analysis of the four-chamber cardiac section dynamic images using speck tracking imaging is not limited by angle.[24] Second, measuring fetal cardiac SI using *fetal HQ* is more repeatable, and generally, the fetal heart's dynamic image has more interference factors, such as an irregular fetal position and unpredictable fetal movements. The results show that for dynamic image analysis, *fetal HQ* has a success rate of 95.4% and an ICC of >0.9, which indicates high consistency. Moreover, the CV was >1%, indicating low variability, and the reproducibility was good.

This study has limitations. First, fetuses in the CoA group had other intracardiac malformations, such as ventricular septal defect and foramen ovale blood flow restriction, which may affect the results. Because this group's sample size was small, it was not possible to subgroup the cases for a more detailed comparison. Future studies with large sample sizes are needed to validate this study's conclusions. Second, LVOTO is associated with similar heart hemodynamic changes and therefore similar ventricle and overall heart shape changes. However, further research is needed to determine the impact of specific LVOTO types on each ventricle segment. This study only involved fetuses with CoA, and in the future, LVOTO should be investigated to identify more strategies for the clinical diagnosis of CoA. Third, the main *fetal HQ* analysis section is the 2D dynamic 4CV, which has high requirements and its accuracy can be affected by many factors, including the thickness of the abdominal wall fat layer in pregnant women, GA, fetal position, amniotic fluid, and the collector's experience. Fourth, the use of the fetal *HQ* software requires specialized knowledge and training.

Conclusion

This study revealed no significant correlation between fetal GA and GSI, LV-FAC, LV-GLS, RV-FAC, and RV-GL in the CoA and control groups. However, in fetuses with CoA, GSI was decreased and the overall heart shape was close to spherical. In fetuses with CoA, the left ventricular diameter was decreased, the apical segment's SI was increased, and the ventricular morphology tended to be flattened. The right ventricle's transverse diameter was increased, while the spherical index of some basal segments, all intermediate segments, and apical segments was decreased, resulting in a more spherical ventricular morphology. In fetuses with CoA, the left ventricle's global, transverse, and longitudinal systolic functions were reduced, and the right ventricle's global and longitudinal systolic functions were also reduced, whereas its lateral systolic function was reduced in the basal and intermediate segments. *Fetal HQ*, a new simple technique that offers rapid analysis and high repeatability, can quantitatively evaluate changes in fetal heart structure and systolic function.

Funding

The study was funded by the Ningxia Natural Science Foundation (grant ID. 2022A1467).

Author Contributions

Jiaojiao Yang and Xueqin Ji contributed to the conception and design of the study. Fang Tan and Yuqin Shen contributed to data interpretation and drafted the manuscript. Yuan Zhao, Yan Xia and Sihan Fan contributed to data analysis and data acquisition. The authors read and approved the final manuscript.

Conflicts of Interest

None.

Data Availability

The datasets used and/or analyzed during the current study are available from the corresponding author on request.

References

[1] Jacobs ML. Congenital heart surgery nomenclature and database project: truncus arteriosus. Ann Thorac Surg 2000;69(4 Suppl):S50–S55. doi: 10.1016/s0003-4975(99)01320-x.
[2] Mitchell SC, Korones SB, Berendes HW. Congenital heart disease in 56,109 births. Incidence and natural history. Circulation 1971; 43(3):323–332. doi: 10.1161/01.cir.43.3.323.
[3] Lytzen R, Vejlstrup N, Bjerre J, et al. Live-born major congenital heart disease in Denmark: incidence, detection rate, and termination of pregnancy rate from 1996 to 2013. JAMA Cardiol 2018;3(9):829–837. doi: 10.1001/jamacardio.2018.2009.
[4] Bjornard K, Riehle-Colarusso T, Gilboa SM, et al. Patterns in the prevalence of congenital heart defects, metropolitan Atlanta, 1978 to 2005. Birth Defects Res A Clin Mol Teratol 2013;97(2):87–94. doi: 10.1002/bdra.23111.
[5] Campbell M. Natural history of coarctation of the aorta. Br Heart J 1970;32(5):633–640. doi: 10.1136/hrt.32.5.633.
[6] Obstetrics and Gynecology Ultrasound Group, Ultrasound Medicine Branch of Chinese Medical Association. Chinese expert consensus on ultrasound examination of fetal aorta (2022 edition) (in Chinese). Chin J Ultrasound Imaging 2022;31(03):203–207. doi: 10.3760/cma.j.cn131148-20220104-00007.
[7] Li W, Zhao B, Pan M, et al. A preliminary study of 24-segment spherical indexes of fetal ventricles in the middle and late trimestries by automatic fetal heart quantification (in Chinese). Chin J Ultrasound Imaging 2020; 29(07):586–591. doi: 10.3760/cma.j.cn131148-20191226-00800.
[8] DeVore GR, Satou G, Sklansky M. Area of the fetal heart's four-chamber view: a practical screening tool to improve detection of cardiac abnormalities in a low-risk population. Prenat Diagn 2017;37(2): 151–155. doi: 10.1002/pd.4980.
[9] DeVore GR. Computing the Z score and centiles for cross-sectional analysis: a practical approach. J Ultrasound Med 2017;36(3): 459–473. doi: 10.7863/ultra.16.03025.
[10] DeVore GR, Satou G, Sklansky M. Abnormal fetal findings associated with a global sphericity index of the 4-chamber view below the 5th centile. J Ultrasound Med 2017;36(11):2309–2318. doi: 10.1002/jum.14261.
[11] DeVore GR, Klas B, Satou G, et al. Evaluation of the right and left ventricles: an integrated approach measuring the area, length, and width of the chambers in normal fetuses. Prenat Diagn 2017;37(12): 1203–1212. doi: 10.1002/pd.5166.

[12] DeVore GR, Klas B, Satou G, et al. 24-segment sphericity index: a new technique to evaluate fetal cardiac diastolic shape. Ultrasound Obstet Gynecol 2018;51(5):650–658. doi: 10.1002/uog.17505.
[13] DeVore GR, Klas B, Satou G, et al. Longitudinal annular systolic displacement compared to global strain in normal fetal hearts and those with cardiac abnormalities. J Ultrasound Med 2018;37(5):1159–1171. doi: 10.1002/jum.14454.
[14] DeVore GR, Klas B, Satou G, et al. Twenty-four segment transverse ventricular fractional shortening: a new technique to evaluate fetal cardiac function. J Ultrasound Med 2018;37(5):1129–1141. doi: 10.1002/jum.14455.
[15] DeVore GR, Zaretsky M, Gumina DL, et al. Right and left ventricular 24-segment sphericity index is abnormal in small-for-gestational-age fetuses. Ultrasound Obstet Gynecol 2018;52(2):243–249. doi: 10.1002/uog.18820.
[16] DeVore GR, Klas B, Satou G, et al. Quantitative evaluation of fetal right and left ventricular fractional area change using speckle-tracking technology. Ultrasound Obstet Gynecol 2019;53(2):219–228. doi: 10.1002/uog.19048.
[17] DeVore GR, Klas B, Satou G, et al. Speckle tracking of the basal lateral and septal wall annular plane systolic excursion of the right and left ventricles of the fetal heart. J Ultrasound Med 2019;38(5):1309–1318. doi: 10.1002/jum.14811.
[18] Wu Y, Wang H, Ren J, et al. Effect of fetal four-chamber view on routine prenatal ultrasonographic screening (in Chinese). J Med Imaging Technol 2001;17(09):888–889.
[19] DeVore GR, Klas B, Satou G, et al. Evaluation of fetal left ventricular size and function using speckle-tracking and the Simpson rule. J Ultrasound Med 2019;38(5):1209–1221. doi: 10.1002/jum.14799.
[20] Clavero Adell M, Ayerza Casas A, Jiménez Montañés L, et al. Evolution of strain and strain rate values throughout gestation in healthy fetuses. Int J Cardiovasc Imaging 2020;36(1):59–66. doi: 10.1007/s10554-019-01695-6.
[21] DeVore GR, Jone PN, Satou G, et al. Aortic coarctation: a comprehensive analysis of shape, size, and contractility of the fetal heart. Fetal Diagn Ther 2020;47(5):429–439. doi: 10.1159/000500022.
[22] DeVore GR, Haxel C, Satou G, et al. Improved detection of coarctation of the aorta using speckle-tracking analysis of fetal heart on last examination prior to delivery. Ultrasound Obstet Gynecol 2021;57(2):282–291. doi: 10.1002/uog.21989.
[23] Pang C, Li X, Huang H, et al. The reference range of the fetal global sphericity index Z-score in normal fetus (in Chinese). Chin J Ultrasound Med 2021;37(04):446–449.
[24] Liu X. Application of Fetal HQ to evaluate the morphological and functional changes of ventricles in fetuses with restricted foramen ovale channels in late pregnancy (in Chinese). Shenyang, Liaoning. China Medical University 2023.
[25] Zhan M, Zhao B, Peng X, et al. Investigation of fetal cardiac function and morphology in fetuses with left ventricular outflow tract obstruction using fetal heart quantification (in Chinese). Chin J Ultrasound Imaging 2021;31(10):854–860. doi: 10.3760/cma.j.cn131148-20210406-00242.
[26] Liu J, Cao H, Zhang L, et al. Incremental value of myocardial deformation in predicting postnatal coarctation of the aorta: establishment of a novel diagnostic model. J Am Soc Echocardiogr 2022;35(12):1298–1310. doi: 10.1016/j.echo.2022.07.010.
[27] Stricagnoli M, Cameli M, Incampo E, et al. Speckle tracking echocardiography in cardiac amyloidosis. Heart Fail Rev 2019;24(5):701–707. doi: 10.1007/s10741-019-09796-z.
[28] Stepanova AI, Radova NF, Alekhin MN. Speckle tracking stress echocardiography on treadmill in assessment of the functional significance of the degree of coronary artery disease. Kardiologiia 2021;61(3):4–11. doi: 10.18087/cardio.2021.3.n1462.
[29] Xu L, Huang X, Ma J, et al. Value of three-dimensional strain parameters for predicting left ventricular remodeling after ST-elevation myocardial infarction. Int J Cardiovasc Imaging 2017;33(5):663–673. doi: 10.1007/s10554-016-1053-3.
[30] Luis SA, Chan J, Pellikka PA. Echocardiographic assessment of left ventricular systolic function: An overview of contemporary techniques, including speckle-tracking echocardiography. Mayo Clin Proc 2019;94(1):125–138. doi: 10.1016/j.mayocp.2018.07.017.
[31] Cameli M, Mandoli GE, Sciaccaluga C, et al. More than 10 years of speckle tracking echocardiography: Still a novel technique or a definite tool for clinical practice?. Echocardiography 2019;36(5):958–970. doi: 10.1111/echo.14339.
[32] Shen Y, Tan F, Yang J, et al. A preliminary study on fetal cardiac morphology and systolic function of normal and anemic pregnant women by fetal heart quantification technology. Transl Pediatr 2022;11(8):1336–1345. doi: 10.21037/tp-22-315.
[33] Tan F, Yang J, Shen Y, et al. Evaluating fetal heart morphology in hypertensive disorders of pregnancy using the fetal heart quantitative technique. Transl Pediatr 2022;11(11):1804–1812. doi: 10.21037/tp-22-492.
[34] Xu R, Zhou D, Liu Y, et al. Impaired elastic properties of the ascending aorta in fetuses with coarctation of the aorta. J Am Heart Assoc 2023;12(2):e028015. doi: 10.1161/JAHA.122.028015.
[35] Corstius HB, Zimanyi MA, Maka N, et al. Effect of intrauterine growth restriction on the number of cardiomyocytes in rat hearts. Pediatr Res 2005;57(6):796–800. doi: 10.1203/01.PDR.0000157726.65492.CD.
[36] Schipke J, Gonzalez-Tendero A, Cornejo L, et al. Experimentally induced intrauterine growth restriction in rabbits leads to differential remodelling of left versus right ventricular myocardial microstructure. Histochem Cell Biol 2017;148(5):557–567. doi: 10.1007/s00418-017-1587-z.
[37] Cruz-Lemini M, Crispi F, Valenzuela-Alcaraz B, et al. Fetal cardiovascular remodeling persists at 6 months in infants with intrauterine growth restriction. Ultrasound Obstet Gynecol 2016;48(3):349–356. doi: 10.1002/uog.15767.
[38] Crispi F, Miranda J, Gratacós E. Long-term cardiovascular consequences of fetal growth restriction: biology, clinical implications, and opportunities for prevention of adult disease. Am J Obstet Gynecol 2018;218(2S):S869–S879. doi: 10.1016/j.ajog.2017.12.012.
[39] Parra-Saavedra M, Simeone S, Triunfo S, et al. Correlation between histological signs of placental underperfusion and perinatal morbidity in late-onset small-for-gestational-age fetuses. Ultrasound Obstet Gynecol 2015;45(2):149–155. doi: 10.1002/uog.13415.

Edited By Jue Li and Yang Pan

How to cite this article: Yang J, Tan F, Shen Y, Zhao Y, Xia Y, Fan S, Ji X. Assessing Coarctation of the Aorta With Fetal Heart Quantification Technology. Maternal Fetal Med 2024;6(3):147–155. doi: 10.1097/FM9.0000000000000231.